

This discussion paper is/has been under review for the journal Atmospheric Measurement Techniques (AMT). Please refer to the corresponding final paper in AMT if available.

# MIPAS database: new HNO<sub>3</sub> line parameters at 7.6 μm validated with MIPAS satellite measurements

A. Perrin<sup>1</sup>, J.-M. Flaud<sup>1</sup>, M. Ridolfi<sup>2,3</sup>, J. Vander Auwera<sup>4</sup>, and M. Carlotti<sup>5</sup>

<sup>1</sup>Laboratoire Interuniversitaire des Systèmes Atmosphériques (LISA), UMR 7583 CNRS, Universités Paris Est Créteil et Paris Diderot, Institut Pierre Simon Laplace, 61 avenue du Général de Gaulle, 94010 Créteil CEDEX, France

<sup>2</sup>Dipartimento di Fisica e Astronomia, Università di Bologna, 6/2 Viale Berti Pichat, 40127 Bologna, Italia

<sup>3</sup>Istituto di Fisica Applicata “N. Carrara” (IFAC) del Consiglio Nazionale delle Ricerche (CNR), 10 Via Madonna del Piano, 50019 Sesto Fiorentino (FI), Italia

<sup>4</sup>Service de Chimie Quantique et Photophysique, C.P. 160/09, Université Libre de Bruxelles, 50 avenue F.D. Roosevelt, 1050 Brussels, Belgium

<sup>5</sup>Dipartimento di Chimica Industriale “Toso Montanari”, Università di Bologna, 4 Viale del Risorgimento, 40136 Bologna, Italia

**MIPAS database: new HNO<sub>3</sub> line parameters at 7.6 μm validated with MIPAS satellite measurements**

A. Perrin et al.

Title Page

Abstract

Introduction

Conclusions

References

Tables

Figures

◀

▶

◀

▶

Back

Close

Full Screen / Esc

Printer-friendly Version

Interactive Discussion

Received: 23 September 2015 – Accepted: 8 October 2015 – Published: 10 November 2015

Correspondence to: A. Perrin (agnes.perrin@lisa.u-pec.fr)

Published by Copernicus Publications on behalf of the European Geosciences Union.

## AMTD

8, 11643–11671, 2015

### MIPAS database: new $\text{HNO}_3$ line parameters at 7.6 $\mu\text{m}$ validated with MIPAS satellite measurements

A. Perrin et al.

Title Page

Abstract

Introduction

Conclusions

References

Tables

Figures



Back

Close

Full Screen / Esc

Printer-friendly Version

Interactive Discussion



## Abstract

Improved line positions and intensities have been generated for the 7.6  $\mu\text{m}$  spectral region of nitric acid. They were obtained relying on a recent reinvestigation of the nitric acid band system at 7.6  $\mu\text{m}$  and comparisons of  $\text{HNO}_3$  volume mixing ratio profiles retrieved from the “Michelson Interferometer for Passive Atmospheric Sounding” (MIPAS) limb emission radiances in the 11 and 7.6  $\mu\text{m}$  domains. This has led to an improved database called “MIPAS-2015”. Comparisons with available laboratory information (individual line intensities, integrated absorption cross sections, and absorption cross sections) show that MIPAS-2015 provides an improved description of the 7.6  $\mu\text{m}$  region of nitric acid. This study should help to improve  $\text{HNO}_3$  satellite retrievals by allowing measurements to be performed simultaneously in the 11 and 7.6  $\mu\text{m}$  micro-windows. In particular, it should be useful to analyze existing MIPAS and IASI spectra as well as spectra to be recorded by the forthcoming “Infrared Atmospheric Sounding Interferometer – New Generation” (IASI-NG) instrument.

## 1 Introduction

Optical remote sensing of nitric acid in the infrared range can be performed using the three strongest band systems of this species, namely the  $\{\nu_5, 2\nu_9\}$ ,  $\{\nu_3, \nu_4\}$  and  $\nu_2$  band systems located near 11, 7.6 and 5.8  $\mu\text{m}$  respectively. Focusing on the spectral ranges covered by the Michelson Interferometer for Passive Atmospheric Sounding (MIPAS) instrument (Fischer et al., 2008) that was operational on board the ENVISAT satellite (Endemann, 1999) in the years from 2002 to 2012, Flaud et al. (2006 and references therein) created a  $\text{HNO}_3$  linelist covering the 600–1800  $\text{cm}^{-1}$  region with the aim to provide the best and most consistent possible set of line parameters (positions, intensities and shape-specific) for this molecular species. Subsequent laboratory and theoretical studies (Gomez et al., 2009; Laraia et al., 2009) revisited this linelist. The updated linelist thus produced and validated (Tran et al., 2009) is implemented in the

## MIPAS database: new $\text{HNO}_3$ line parameters at 7.6 $\mu\text{m}$ validated with MIPAS satellite measurements

A. Perrin et al.

Title Page

Abstract

Introduction

Conclusions

References

Tables

Figures

◀

▶

◀

▶

Back

Close

Full Screen / Esc

Printer-friendly Version

Interactive Discussion







### 3 The MIPAS-2015 linelist with intensities at 7.6 $\mu\text{m}$ calibrated using $\text{HNO}_3$ retrievals from MIPAS radiances at 11 and 7.6 $\mu\text{m}$

Following the work of (Perrin, 2013), we have generated a list of line positions and relative line intensities for the 7.6  $\mu\text{m}$  region of the spectrum of nitric acid. It includes (see Table 1) the  $\nu_3$  and  $\nu_4$  cold bright bands, the  $2\nu_6$ ,  $3\nu_9$ ,  $\nu_5 + \nu_9$ ,  $\nu_7 + \nu_8$  cold weak bands, and the  $\nu_3 + \nu_9 - \nu_9$  hot band of the main isotopologue. Line shape parameters (air- and self-broadening coefficients, temperature dependence of the air-broadening coefficient, and air-shift coefficients) were added using the corresponding information available in MIPAS-OLD for the 11  $\mu\text{m}$  spectral range of  $\text{HNO}_3$  (Rothman et al., 20012). The  $\text{HNO}_3$  linelist at 7.6  $\mu\text{m}$  of the MIPAS-OLD database was completely replaced by the new linelist, leading to the so-called “MIPAS-2015” linelist. The remainder of MIPAS-OLD was left unchanged.

Using MIPAS radiances, an absolute intensity calibration was performed to “convert” the relative line intensities at 7.6  $\mu\text{m}$  to absolute intensities. More precisely, this was done by comparing  $\text{HNO}_3$  VMR retrieved from MIPAS radiances using the MIPAS-2015 linelist in either the 7.6 or the 11  $\mu\text{m}$  regions. A multiplicative factor was applied to all the line intensities at 7.6  $\mu\text{m}$  so that the  $\text{HNO}_3$  VMR retrieved using the 7.6  $\mu\text{m}$  region matches that retrieved using the 11  $\mu\text{m}$  range. The spectral micro-windows (MWs) selected for the two test retrievals are listed in Table 2. The left panel of Fig. 1 shows averages of 929  $\text{HNO}_3$  VMR profiles retrieved from the MIPAS limb scanning measurements acquired on 24 January 2003 with a FTS spectral resolution of  $0.025 \text{ cm}^{-1}$ . The inversion algorithm adopted for these tests is the so called Optimized Retrieval Model (ORM) version 7.0, that is the scientific prototype of the code used by the European Space Agency (ESA) for routine MIPAS data processing (Ridolfi et al., 2000; Raspollini et al., 2006, 2013). In this test, the profiles are retrieved using the MIPAS-2015 linelist and MWs, alternatively in the 11  $\mu\text{m}$  region (red line) or in the 7.6  $\mu\text{m}$  region (blue line). Being the average of a large number of profiles, the noise error bars are not visible in the plot. We notice that the profiles retrieved from the two spectral regions are in

## MIPAS database: new $\text{HNO}_3$ line parameters at 7.6 $\mu\text{m}$ validated with MIPAS satellite measurements

A. Perrin et al.

Title Page

Abstract

Introduction

Conclusions

References

Tables

Figures



Back

Close

Full Screen / Esc

Printer-friendly Version

Interactive Discussion



---

**MIPAS database: new  
HNO<sub>3</sub> line parameters  
at 7.6 μm validated  
with MIPAS satellite  
measurements**A. Perrin et al.

---

[Title Page](#)[Abstract](#)[Introduction](#)[Conclusions](#)[References](#)[Tables](#)[Figures](#)[◀](#)[▶](#)[◀](#)[▶](#)[Back](#)[Close](#)[Full Screen / Esc](#)[Printer-friendly Version](#)[Interactive Discussion](#)

excellent agreement. To better quantify the residual discrepancies, in the right panel of Fig. 1 we show the percentage differences (black line) between the average profiles retrieved using MWs in the 7.6 and in the 11 μm region. The error bars of the black line represent the statistical error of the mean difference. At each altitude, this error is calculated as the standard deviation of the profile differences divided by the square root of the number of samples at the considered altitude. Note that, especially in the altitude range from 15 to 30 km, where the individual profile retrievals are more stable due to the larger sensitivity of the limb measurements to the HNO<sub>3</sub> amount, the maximum bias between the average profiles is less than 0.8%. Being the average of a large number of profiles, the noise error on the evaluated bias (error bars of the black line of Fig. 1) is rather small. An additional error on the evaluated bias could arise from the inter-band radiometric calibration error in the used MIPAS spectra (Kleinert et al., 2007). The radiometric calibration of MIPAS spectra is constant within the set of measurements considered in the tests of Fig. 1. However, since it is renewed on a weekly basis, to evaluate the impact of this error source in the calibration of the HNO<sub>3</sub> linelist in the 7.6 μm region, we repeated the test illustrated in Fig. 1 with different sets of MIPAS measurements with different radiometric calibrations. We selected MIPAS measurements acquired in three different days of the years 2002 and 2003 (still measurements acquired with the MIPAS full spectral resolution of 0.025 cm<sup>-1</sup>). The results of these additional tests show that, actually, the observed differences between the average HNO<sub>3</sub> VMR retrieved from the 11 and the 7.6 μm regions amount to a maximum of 1.5% in the height range from 15 to 30 km. This is the accuracy we attribute to our HNO<sub>3</sub> linelist calibration procedure. The blue and red lines in the right panel of Fig. 1 indicate the ± noise error of an individual profile retrieval determined from the covariance matrix of the Levenberg–Marquardt inversion method (Ceccherini et al., 2010). While the inversion with the MWs in the 11 μm region provides a smaller retrieval error below 23 km, the MWs in the 7.6 μm region provide a smaller error above 30 km. This behavior is due to the larger intensity of the HNO<sub>3</sub> band system in the 7.6 μm region, the effect of







---

**MIPAS database: new  
HNO<sub>3</sub> line parameters  
at 7.6 μm validated  
with MIPAS satellite  
measurements**

---

A. Perrin et al.

[Title Page](#)[Abstract](#)[Introduction](#)[Conclusions](#)[References](#)[Tables](#)[Figures](#)[◀](#)[▶](#)[◀](#)[▶](#)[Back](#)[Close](#)[Full Screen / Esc](#)[Printer-friendly Version](#)[Interactive Discussion](#)

ties reported in these two studies and those included in the MIPAS-2015 database was limited to well identified and unblended lines. Table 4 presents the averages of the ratios  $R = \text{Int}(\text{MIPAS-2015}) / \text{Int}(\text{Obs})$  of line intensities in MIPAS-2015 with the corresponding measured values. It shows that, on average, the line intensities of MIPAS-2015 are about 37 % weaker and 39 % stronger than measured by May and Webster (1989) and Perrin et al. (1993), respectively.

In view of these diverging results, we decided to measure individual line intensities for nitric acid using a Fourier transform spectrum recorded in Giessen in 2002 (Perrin et al., 2004). This spectrum was recorded in the 718–1436 cm<sup>-1</sup> spectral region at 299.7 K, at a pressure of 0.03 hPa and with an absorption path length of 302 cm (more details can be found in Perrin et al., 2004). Assuming a Gaussian line profile and including instrumental effects arising from the maximum optical path difference of 542 cm and the 1.3 mm entrance aperture used, 348 line intensities were measured for well isolated lines in the 7.6 μm region using the program “WSpectra” (Carleer et al., 2001). Figure 6 presents an overview of the comparison between these measured line intensities and those available in MIPAS-2015.

No clear trend with respect to line positions or line intensities is noticeable. On average, the intensities quoted in MIPAS-2015 are only 5 % smaller than those measured during the present investigation. As shown in Table 4, this corresponds to a much better agreement than with previous works, although this is not a definite confirmation of the accuracy of the line intensities in MIPAS-2015 because the uncertainty of measurement of the HNO<sub>3</sub> pressure for the Giessen spectrum is not precisely known. It is worth noting that large variations of the ratio  $R$  are observed, as shown in Fig. 6; they reflect in the standard deviation on  $R$  which is rather large. Similar behaviors were observed for the other two sets of line by line intensity measurements (May and Webster, 1989; Perrin et al., 1993). Possible explanations of these rather large standard deviations include the fact that it is not always possible to avoid blended lines in the congested 7.6 μm spectral region, even if care was taken to avoid them, and that the theoretical

model used to compute the line intensities is still imperfect, as discussed in details in Perrin (2013).

## 4.2 Integrated band intensities

Flaud et al. (2006) reviewed the integrated band intensities reported in the literature at 11 and 7.6  $\mu\text{m}$  (Goldman et al., 1971; Giver et al., 1984; Massie et al., 1985; Hjorth et al., 1987; Chackerian et al., 2003). As shown in Table 5, these literature results are in reasonable agreement with each other.

As measured integrated band intensities include the contributions of hot bands and bands from isotopologues other than  $\text{H}^{14}\text{N}^{16}\text{O}_3$ , comparison of the experimental integrated band intensities with the sum of the individual line intensities listed in the MIPAS databases require use of the following expression (see Appendix A of Flaud et al., 2006 and Rotger et al., 2008):

$$S_{\text{band}}(T) \approx \frac{Z_{\text{vib}}(T)}{I_a} \sum_k S_k, \quad (1)$$

where  $S_k$  is the intensity of line  $k$  in the MIPAS database accounting for the isotopic abundance,  $Z_{\text{vib}}(T)$  is the vibrational partition function of  $\text{H}^{14}\text{N}^{16}\text{O}_3$  [ $Z_{\text{vib}}(296\text{ K}) = 1.29952$ ] and  $I_a = 0.989$  is its isotopic abundance. The summation in Eq. (1) runs over all the lines of all the cold bands listed in Table 3. In Table 5, the integrated band intensities calculated using MIPAS-OLD and MIPAS-2015 with Eq. (1) are compared with the experimental values reported for the 11 and 7.6  $\mu\text{m}$  regions showing that MIPAS-2015 is in reasonable agreement with the measurements.

## 4.3 Absorption cross sections

We also performed direct comparisons with the experimental absorption cross sections available in the Pacific Northwest National Laboratory (PNNL) library (Sharpe et al., 2004).

### MIPAS database: new $\text{HNO}_3$ line parameters at 7.6 $\mu\text{m}$ validated with MIPAS satellite measurements

A. Perrin et al.

Title Page

Abstract

Introduction

Conclusions

References

Tables

Figures

◀

▶

◀

▶

Back

Close

Full Screen / Esc

Printer-friendly Version

Interactive Discussion





## References

- Carleer, M. R.: WSpectra: a Windows program to accurately measure the line intensities of high-resolution Fourier transform spectra, in: Remote Sensing of Clouds and the Atmosphere V, edited by: Russel, J. E., Schäfer, K., and Lado-Bordowsky, O., Proceedings of SPIE – The International Society for Optical Engineering, 4168, Barcelona, Spain, 337–342, 2001.
- Ceccherini, S. and Ridolfi, M.: Technical Note: Variance-covariance matrix and averaging kernels for the Levenberg-Marquardt solution of the retrieval of atmospheric vertical profiles, Atmos. Chem. Phys., 10, 3131–3139, doi:10.5194/acp-10-3131-2010, 2010.
- Chackerian, C., Sharpe, S. W., and Blake, T. A.: Anhydrous nitric acid integrated absorption cross sections: 820–5300  $\text{cm}^{-1}$ , J. Quant. Spectrosc. Ra., 81, 429–441, 2003.
- Endemann, M.: MIPAS instrument concept and performance, in: Proceedings of the ESAMS'99, 18–22 January 1999, Noordwijk, the Netherlands, ESTEC-ESA, WPP-161, 1, 29–43, ISSN 1022-6656, 1999.
- Flaud, J.-M., Perrin, A., Orphal, J., Kou, Q., Flaud, P.-M., Dutkiewicz, Z., and Piccolo, C.: New analysis of the  $\nu_5 + \nu_9 - \nu_9$  hot band of  $\text{HNO}_3$ , J. Quant. Spectrosc. Ra., 77, 355–364, 2003.
- Flaud, J.-M., Brizzi, G., Carlotti, M., Perrin, A., and Ridolfi, M.: MIPAS database: Validation of  $\text{HNO}_3$  line parameters using MIPAS satellite measurements, Atmos. Chem. Phys., 6, 5037–5048, doi:10.5194/acp-6-5037-2006, 2006.
- Fischer, H., Birk, M., Blom, C., Carli, B., Carlotti, M., von Clarmann, T., Delbouille, L., Dudhia, A., Ehhalt, D., Endemann, M., Flaud, J. M., Gessner, R., Kleinert, A., Koopman, R., Langen, J., López-Puertas, M., Mosner, P., Nett, H., Oelhaf, H., Perron, G., Remedios, J., Ridolfi, M., Stiller, G., and Zander, R.: MIPAS: an instrument for atmospheric and climate research, Atmos. Chem. Phys., 8, 2151–2188, doi:10.5194/acp-8-2151-2008, 2008.
- Giver, L. P., Valero, F. P. J., Goorvitch, D., and Bonomo, F. S.: Nitric-acid band intensities and band-model parameters from 610 to 1760  $\text{cm}^{-1}$ , J. Opt. Soc. Am. B, 1, 715–722, 1984.
- Goldman, A., Kyle, T. G., and Bonomo, F. S.: Statistical band model parameters and integrated intensities for the 5.9- $\mu\text{m}$ , 7.5- $\mu\text{m}$ , and 11.3- $\mu\text{m}$  bands of  $\text{HNO}_3$  vapor, Appl. Optics, 10, 65–73, 1971.
- Goldman, A., Rinsland, C. P., Perrin, A., and Flaud, J.-M.:  $\text{HNO}_3$  line parameters: 1996 HITRAN update and new results, J. Quant. Spectrosc. Ra., 60, 851–861, 1998.

## MIPAS database: new $\text{HNO}_3$ line parameters at 7.6 $\mu\text{m}$ validated with MIPAS satellite measurements

A. Perrin et al.

Title Page

Abstract

Introduction

Conclusions

References

Tables

Figures

◀

▶

◀

▶

Back

Close

Full Screen / Esc

Printer-friendly Version

Interactive Discussion





**MIPAS database: new  
HNO<sub>3</sub> line parameters  
at 7.6 μm validated  
with MIPAS satellite  
measurements**

A. Perrin et al.

Title Page

Abstract

Introduction

Conclusions

References

Tables

Figures

◀

▶

◀

▶

Back

Close

Full Screen / Esc

Printer-friendly Version

Interactive Discussion



May, R. D. and Webster, C. R.: Measurements of line positions, intensities, and collisional air broadening coefficients in the HNO<sub>3</sub> 7.5 μm band using a computed – controlled tunable diode laser spectrometer, *J. Mol. Spectrosc.*, 138, 383–397, 1989.

Mencaraglia, F., Bianchini, G., Boscaleri, A., Carli, B., Ceccherini, S., Raspollini, P., Perrin, A., and Flaud, J.-M.: Validation of MIPAS satellite measurements of HNO<sub>3</sub> using comparison of rotational and vibrational spectroscopy, *J. Geophys. Res.*, 111, D19305, doi:10.1029/2005JD006099, 2006.

Perrin, A.: New analysis of the ν<sub>3</sub> and ν<sub>4</sub> bands of HNO<sub>3</sub> in the 7.6 μm region, *J. Phys. Chem. A*, 117, 13236–13248, 2013.

Perrin, A., Lado-Bordowski, O., and Valentin, A.: The ν<sub>3</sub> and ν<sub>4</sub> interacting bands of HNO<sub>3</sub> line positions and line intensities, *Mol. Phys.*, 67, 249–270, 1989.

Perrin, A., Flaud, J.-M., Camy-Peyret, C., Jaouen, V., Farrenq, R., Guelachvili, G., Kou, Q., Le Roy, F., Morillon-Chapey, M., Orphal, J., Badaoui, M., Mandin, J.-Y., and Dana, V.: Line intensities in the 11- and 7.6-μm bands on HNO<sub>3</sub>, *J. Mol. Spectrosc.*, 160, 524–539, 1993.

Perrin, A., Orphal, J., Flaud, J.-M., Klee, S., Mellau, G., Mäder, H., Walbrodt, D., and Winnewisser, M.: New analysis of the ν<sub>5</sub> and 2ν<sub>9</sub> bands of HNO<sub>3</sub> by infrared and millimeter wave techniques: line positions and intensities, *J. Mol. Spectrosc.*, 228, 375–391, 2004.

Raspollini, P., Belotti, C., Burgess, A., Carli, B., Carlotti, M., Ceccherini, S., Dinelli, B. M., Dudhia, A., Flaud, J.-M., Funke, B., Höpfner, M., López-Puertas, M., Payne, V., Piccolo, C., Remedios, J. J., Ridolfi, M., and Spang, R.: MIPAS level 2 operational analysis, *Atmos. Chem. Phys.*, 6, 5605–5630, doi:10.5194/acp-6-5605-2006, 2006.

Raspollini, P., Carli, B., Carlotti, M., Ceccherini, S., Dehn, A., Dinelli, B. M., Dudhia, A., Flaud, J.-M., López-Puertas, M., Niro, F., Remedios, J. J., Ridolfi, M., Sembhi, H., Sgheri, L., and von Clarmann, T.: Ten years of MIPAS measurements with ESA Level 2 processor V6 – Part 1: Retrieval algorithm and diagnostics of the products, *Atmos. Meas. Tech.*, 6, 2419–2439, doi:10.5194/amt-6-2419-2013, 2013.

Ridolfi, M., Carli, B., Carlotti, M., von Clarmann, T., Dinelli, B. M., Dudhia, A., Flaud, J.-M., Hoepfner, M., Morris, P. E., Raspollini, P., Stiller, G., and Wells, R. J.: Optimized forward model and retrieval scheme for MIPAS near-real-time data processing, *Appl. Optics*, 39, 1323–1340, 2000.

Rotger, M., Boudon, V., and Vander Auwera J.: Line positions and intensities in the ν<sub>12</sub> band of ethylene near 1450 cm<sup>-1</sup>: an experimental and theoretical study, *J. Quant. Spectrosc. Ra.*, 109, 952–962, 2008.



## MIPAS database: new $\text{HNO}_3$ line parameters at 7.6 $\mu\text{m}$ validated with MIPAS satellite measurements

A. Perrin et al.

Title Page

Abstract

Introduction

Conclusions

References

Tables

Figures

◀

▶

◀

▶

Back

Close

Full Screen / Esc

Printer-friendly Version

Interactive Discussion



Rothman, L. S., Gordon, I. E., Barbe, A., Chris Benner, D., Bernath, P. F., Birk, M., Boudon, V., Brown, L. R., Campargue, A., Champion, J.-P., Chance, K., Coudert, L. H., Dana, V., Devi, V. M., Fally, S., Flaud, J.-M., Gamache, R. R., Goldman, A., Jacquemart, D., Kleiner, I., Lacombe, N., Lafferty, W. J., Mandin, J.-Y., Massie, S. T., Mikhailenko, S. N., Miller, C. E.,  
 5 Moazzen-Ahmadi, N., Naumenko, O. V., Nikitin, A. V., Orphal, J., Perevalov, V. I., Perrin, A., Predoi-Cross, A., Rinsland, C. P., Rotger, M., Simeckova, M., Smith, M. A. H., Sung, K., Tashkun, S. A., Tennyson, J., Toth, R. A., Vandaele, A. C., and Vander Auwera, J.: The HITRAN 2008 molecular spectroscopic database, *J. Quant. Spectrosc. Ra.*, 110, 533–572, 2009.

Rothman, L. S., Gordon, I. E., Babikov, Y., Barbe, A., Chris Benner, D., Bernath, P. F., Birk, M., Bizzocchi, L., Boudon, V., Brown, L. R., Campargue, A., Chance, K., Cohen, E. A., Coudert, L. H., Devi, V. M., Drouin, B. J., Fayt, A., Flaud, J.-M., Gamache, R. R., Harrison, J. J., Hartmann, J.-M., Hill, C., Hodges, J. T., Jacquemart, D., Jolly, A., Lamouroux, J., Le Roy, R. J., Li, G., Long, D. A., Lyulin, O. M., Mackie, C. J., Massie, S. T., Mikhailenko, S.,  
 10 Müller, H. S. P., Naumenko, O. V., Nikitin, A. V., Orphal, J., Perevalov, V., Perrin, A., Polovtseva, E. R., Richard, C., Smith, M. A. H., Starikova, E., Sung, K., Tashkun, S., Tennyson, J., Toon, G. C., Tyuterev, V. I. G., and Wagner, G.: The HITRAN2012 Molecular Spectroscopic Database, *J. Quant. Spectrosc. Ra.*, 130, 4–50, 2013.

Sharpe, S. W., Johnson, T. J., Sams, R. L., Chu, P. M., Rhoderick, G. C., and Johnson, P. A.: Gas-phase databases for quantitative infrared spectroscopy, *Appl. Spectrosc.*, 58, 1452–1465, 2004.

Tran, H., Brizzi, G., Gomez, L., Perrin, A., Hase, F., Ridolfi, M., and Hartmann, J. M.: Validation of  $\text{HNO}_3$  spectroscopic parameters using atmospheric absorption and emission measurements, *J. Quant. Spectrosc. Ra.*, 110, 109–117, 2009.

Wespes, C., Hurtmans, D., Clerbaux, C., Santee, M. L., Martin, R. V., and Coheur, P. F.: Global distributions of nitric acid from IASI/MetOP measurements, *Atmos. Chem. Phys.*, 9, 7949–7962, doi:10.5194/acp-9-7949-2009, 2009.

Wang, D. Y., Höpfner, M., Blom, C. E., Ward, W. E., Fischer, H., Blumenstock, T., Hase, F., Keim, C., Liu, G. Y., Mikuteit, S., Oelhaf, H., Wetzel, G., Cortesi, U., Mencaraglia, F., Bianchini, G., Redaelli, G., Pirre, M., Catoire, V., Huret, N., Vigouroux, C., De Mazière, M., Mahieu, E., Demoulin, P., Wood, S., Smale, D., Jones, N., Nakajima, H., Sugita, T., Urban, J., Murtagh, D., Boone, C. D., Bernath, P. F., Walker, K. A., Kuttippurath, J., Kleinböhl, A.,  
 30



Toon, G., and Piccolo, C.: Validation of MIPAS HNO<sub>3</sub> operational data, Atmos. Chem. Phys., 7, 4905–4934, doi:10.5194/acp-7-4905-2007, 2007.

Wolff, M. A., Kerzenmacher, T., Strong, K., Walker, K. A., Toohey, M., Dupuy, E., Bernath, P. F., Boone, C. D., Brohede, S., Catoire, V., von Clarmann, T., Coffey, M., Daffer, W. H., De Maz-  
5 ière, M., Duchatelet, P., Glatthor, N., Griffith, D. W. T., Hannigan, J., Hase, F., Höpfner, M., Huret, N., Jones, N., Jucks, K., Kagawa, A., Kasai, Y., Kramer, I., Küllmann, H., Kuttippu-  
rath, J., Mahieu, E., Manney, G., McElroy, C. T., McLinden, C., Mébarki, Y., Mikuteit, S.,  
Murtagh, D., Piccolo, C., Raspollini, P., Ridolfi, M., Ruhnke, R., Santee, M., Senten, C.,  
10 Smale, D., Tétard, C., Urban, J., and Wood, S.: Validation of HNO<sub>3</sub>, ClONO<sub>2</sub>, and N<sub>2</sub>O<sub>5</sub> from the Atmospheric Chemistry Experiment Fourier Transform Spectrometer (ACE-FTS), Atmos. Chem. Phys., 8, 3529–3562, doi:10.5194/acp-8-3529-2008, 2008.

## AMTD

8, 11643–11671, 2015

### MIPAS database: new HNO<sub>3</sub> line parameters at 7.6 μm validated with MIPAS satellite measurements

A. Perrin et al.

Title Page

Abstract

Introduction

Conclusions

References

Tables

Figures

◀

▶

◀

▶

Back

Close

Full Screen / Esc

Printer-friendly Version

Interactive Discussion







## MIPAS database: new HNO<sub>3</sub> line parameters at 7.6 μm validated with MIPAS satellite measurements

A. Perrin et al.

**Table 3.** HNO<sub>3</sub> line parameters in the 7.6 μm region.

(a) The MIPAS-OLD database						
Band	NB	$S_{\text{tot}}$ (10 <sup>-18</sup> )	$\sigma_{\text{min}}$	$\sigma_{\text{max}}$	$S_{\text{min}}$ (10 <sup>-23</sup> )	$S_{\text{max}}$ (10 <sup>-21</sup> )
$\nu_3$	21 308	25.37	1098.376	1387.849	1.037	31.33
$\nu_4$	19 584	12.78	1229.867	1387.561	1.037	18.67
Sum		38.15				
(b) The MIPAS-2015 database						
Band	NB	$S_{\text{tot}}$ (10 <sup>-18</sup> )	$\sigma_{\text{min}}$	$\sigma_{\text{max}}$	$S_{\text{min}}$ (10 <sup>-25</sup> )	$S_{\text{max}}$ (10 <sup>-21</sup> )
$\nu_3$	16 408	24.940	1252.010	1387.081	4.910	32.0
$\nu_4$	18 105	9.834	1238.929	1387.561	4.020	21.4
$2\nu_6$	2451	0.119	1243.465	1348.275	4.624	3.660
$\nu_5 + \nu_9$	13 817	0.716	1246.929	1390.071	2.081	3.543
$\nu_7 + \nu_8$	11 125	0.761	1246.422	1395.679	2.314	5.017
$3\nu_9$	13 894	1.177	1233.107	1388.497	4.582	2.378
Sum		37.547				
$\nu_3 + \nu_9 - \nu_9$	12 106	1.408	1271.050	1394.899	5.285	1.798

NB is the number of lines,  $\sigma_{\text{min}}$  and  $\sigma_{\text{max}}$  (cm<sup>-1</sup>) give the wavenumber range of the bands,  $S_{\text{min}}$  and  $S_{\text{max}}$  are the smallest and largest line intensity in cm<sup>-1</sup> (molecule cm<sup>2</sup>)<sup>-1</sup> at 296 K,  $S_{\text{tot}}$  is the sum of the line intensities in cm<sup>-1</sup> (molecule cm<sup>2</sup>)<sup>-1</sup> at 296 K.

## MIPAS database: new HNO<sub>3</sub> line parameters at 7.6 μm validated with MIPAS satellite measurements

A. Perrin et al.

**Table 4.** Average ratios  $R_{\text{mean}}$  of line intensities included in MIPAS-2015 (at 296 K) and measured in the literature and in this work.

Report	#	$R_{\text{mean}}$
May and Webster (1989) (296 K)	256	0.73 (21)
Perrin et al. (1993) (271 K)	40	1.39 (21)
This work (299.7 K)	348	0.95 (18)

The comparison accounts for the temperature conversion to 296 K, # is the number of line intensities included in the average. The numbers between parentheses are the standard deviations, in the units of the last digit quoted.

Title Page

Abstract

Introduction

Conclusions

References

Tables

Figures

◀

▶

◀

▶

Back

Close

Full Screen / Esc

Printer-friendly Version

Interactive Discussion



## MIPAS database: new HNO<sub>3</sub> line parameters at 7.6 μm validated with MIPAS satellite measurements

A. Perrin et al.

Title Page

Abstract

Introduction

Conclusions

References

Tables

Figures

◀

▶

◀

▶

Back

Close

Full Screen / Esc

Printer-friendly Version

Interactive Discussion



**Table 5.** Comparison of measured and calculated HNO<sub>3</sub> integrated band intensities in the 11 μm [820–950 cm<sup>-1</sup>] and 7.6 μm [1240–1400 cm<sup>-1</sup>] spectral ranges.

Reference	11 μm $S_{\text{band}}$ (296 K)	7.6 μm $S_{\text{band}}$ (296 K)	7.6 μm/11 μm $R$
Goldman et al. (1971)	2.39 (37)	4.66 (40)	1.95 (47)
Giver et al. (1984)	2.57 (13)	5.15 (16)	2.00 (16)
Massie et al. (1985)	1.98 (30)	3.72 (56)	1.88 (57)
Hjorth et al. (1987)	2.21 (33)	4.29 (60)	1.94 (78)
Chackerian et al. (2003)	2.424 (65)	5.09 (18)	2.10 (13)
PNNL <sup>1</sup> [Sharpe et al. (2004)]	2.538 (85)	5.04 (17)	1.99 (13)
MIPAS-OLD <sup>2</sup> Flaud et al. (2006)	2.335	5.013	2.148
MIPAS-2015 <sup>2</sup> (This work)	2.335	4.934	2.109

All the intensities are given in  $10^{-17} \text{ cm}^{-1} (\text{molecule cm}^2)^{-1}$  at  $T = 296 \text{ K}$ ,  
 $7.6 \mu\text{m}/11 \mu\text{m } R = 7.6 \mu\text{m } S_{\text{band}}(296 \text{ K}) / 11 \mu\text{m } S_{\text{band}}(296 \text{ K})$ .

<sup>1</sup> PNNL: Pacific Northwest National Laboratory.

<sup>2</sup> To estimate the integrated band intensities for MIPAS-OLD and MIPAS-2015, the sums of the cold band intensities (listed in Table 3) are multiplied by 1.314 (see text for details).

## MIPAS database: new $\text{HNO}_3$ line parameters at 7.6 $\mu\text{m}$ validated with MIPAS satellite measurements

A. Perrin et al.

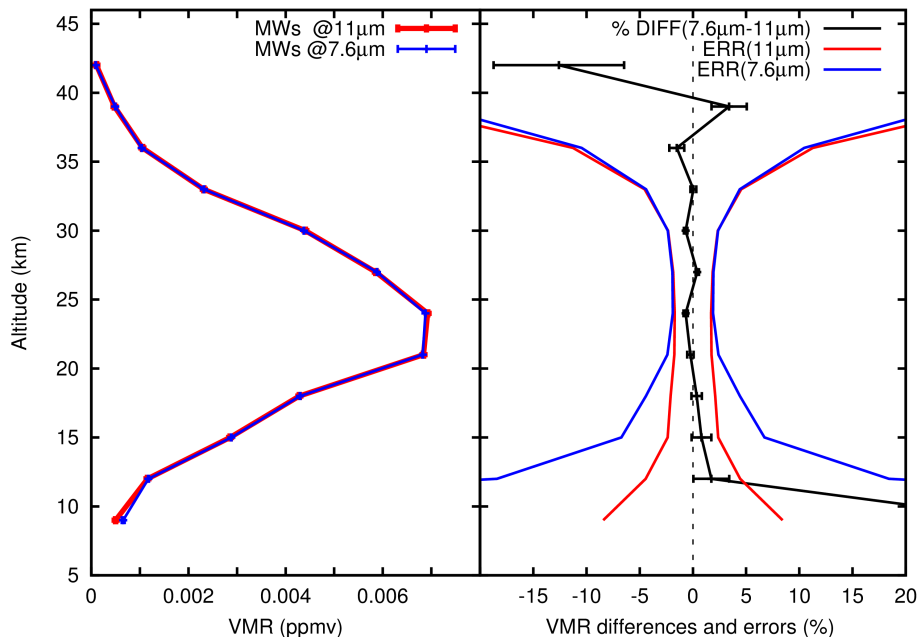


**Figure 1.** Left panel: average  $\text{HNO}_3$  VMR profiles from MIPAS measurements acquired on 24 January 2003, MIPAS-2015 linelist used. Retrievals using MWs in the 11  $\mu\text{m}$  region (red line) and in the 7.6  $\mu\text{m}$  region (blue line). Right panel: mean percentage differences between  $\text{HNO}_3$  profiles retrieved from the 7.6 and 11  $\mu\text{m}$  regions (black line). The red and the blue lines show the noise error of the individual retrievals using MWs in the 11 and in the 7.6  $\mu\text{m}$  spectral regions.

## MIPAS database: new $\text{HNO}_3$ line parameters at 7.6 $\mu\text{m}$ validated with MIPAS satellite measurements

A. Perrin et al.

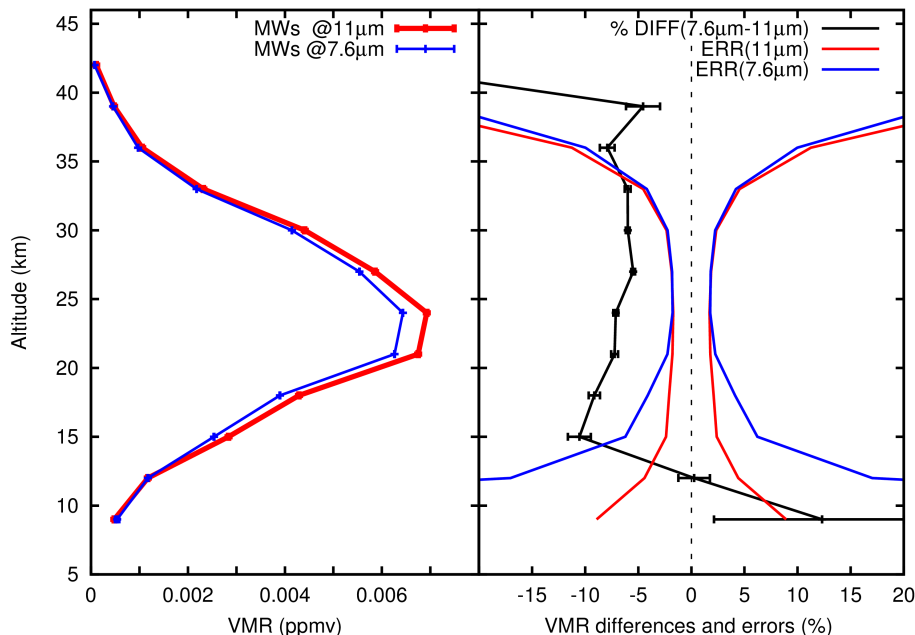


**Figure 2.** Left panel: average  $\text{HNO}_3$  VMR profiles from MIPAS measurements acquired on 24 January 2003, MIPAS-OLD linelist used. Retrievals using MWs in the 11  $\mu\text{m}$  region (red line) and in the 7.6  $\mu\text{m}$  region (blue line). Right panel: mean percentage differences between  $\text{HNO}_3$  profiles retrieved from the 7.6 and 11  $\mu\text{m}$  regions (black line). The red and the blue lines show the noise error of the individual retrievals using MWs in the 11 and in the 7.6  $\mu\text{m}$  spectral regions.

Title Page

Abstract

Introduction

Conclusions

References

Tables

Figures

◀

▶

◀

▶

Back

Close

Full Screen / Esc

Printer-friendly Version

Interactive Discussion



## MIPAS database: new $\text{HNO}_3$ line parameters at 7.6 $\mu\text{m}$ validated with MIPAS satellite measurements

A. Perrin et al.

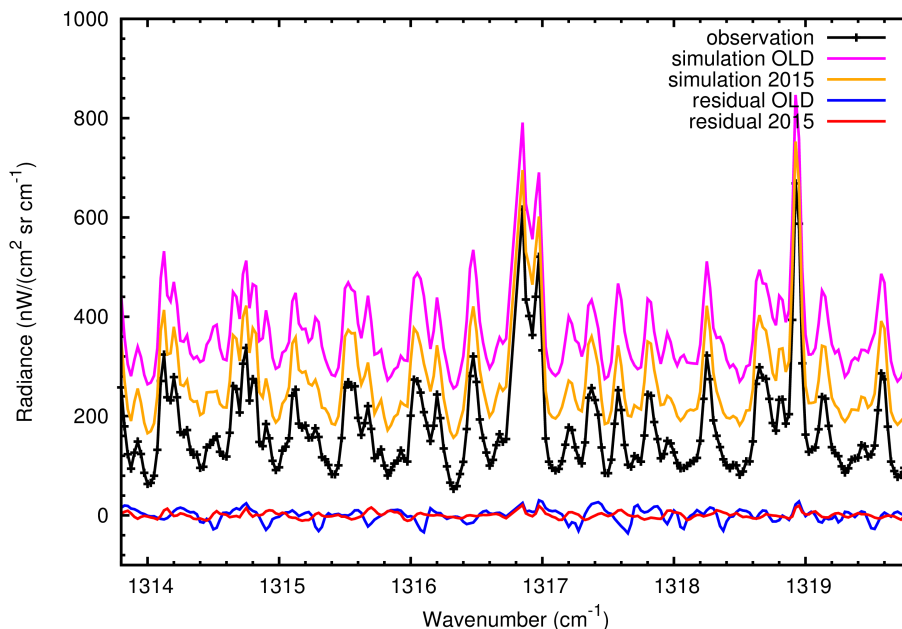


**Figure 3.** Average MIPAS observed spectrum (black) in the 1314–1320  $\text{cm}^{-1}$  spectral region, and spectra simulated with the MIPAS-OLD (magenta line) and the MIPAS-2015 (orange line)  $\text{HNO}_3$  line lists. For better readability of the plot, the average orange and magenta lines were shifted by 100 and 200  $\text{nW}/(\text{cm}^2 \text{sr cm}^{-1})^{-1}$  respectively. The blue and the red lines are the residuals obtained with the MIPAS-OLD and the MIPAS-2015 line lists respectively.

[Title Page](#)[Abstract](#)[Introduction](#)[Conclusions](#)[References](#)[Tables](#)[Figures](#)[◀](#)[▶](#)[◀](#)[▶](#)[Back](#)[Close](#)[Full Screen / Esc](#)[Printer-friendly Version](#)[Interactive Discussion](#)

## MIPAS database: new $\text{HNO}_3$ line parameters at 7.6 $\mu\text{m}$ validated with MIPAS satellite measurements

A. Perrin et al.

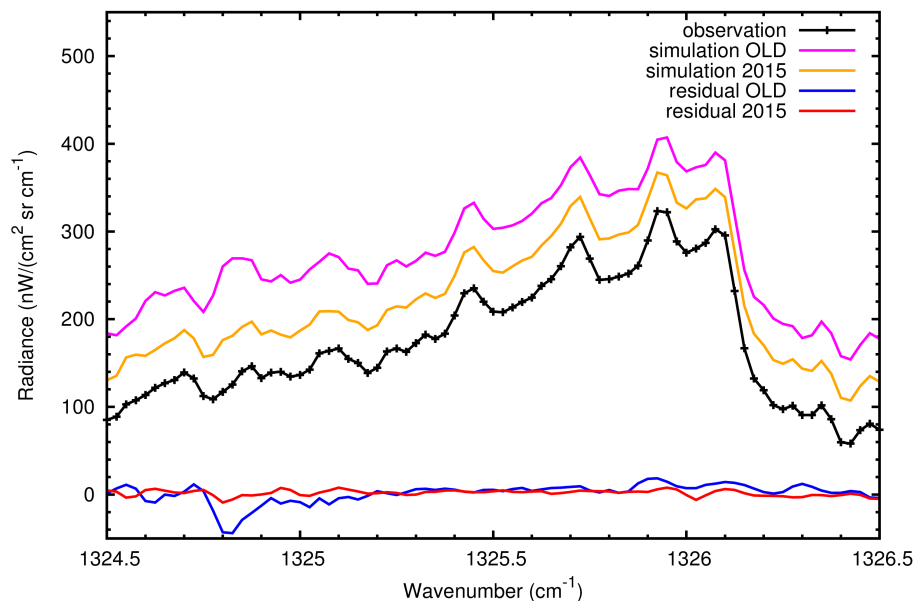


**Figure 4.** Average MIPAS observed spectrum (black) in the 1324.5–1326.5  $\text{cm}^{-1}$  spectral region, and simulated spectra with the MIPAS-OLD (magenta line) and the MIPAS-2015 (orange line)  $\text{HNO}_3$  line lists. For better readability of the plot, the average orange and magenta lines were shifted by 50 and 100  $\text{nW}(\text{cm}^2 \text{sr cm}^{-1})^{-1}$  respectively. The blue and the red lines are the residuals obtained with the MIPAS-OLD and the MIPAS-2015 line lists respectively.

[Title Page](#)[Abstract](#)[Introduction](#)[Conclusions](#)[References](#)[Tables](#)[Figures](#)[◀](#)[▶](#)[◀](#)[▶](#)[Back](#)[Close](#)[Full Screen / Esc](#)[Printer-friendly Version](#)[Interactive Discussion](#)

## MIPAS database: new $\text{HNO}_3$ line parameters at 7.6 $\mu\text{m}$ validated with MIPAS satellite measurements

A. Perrin et al.

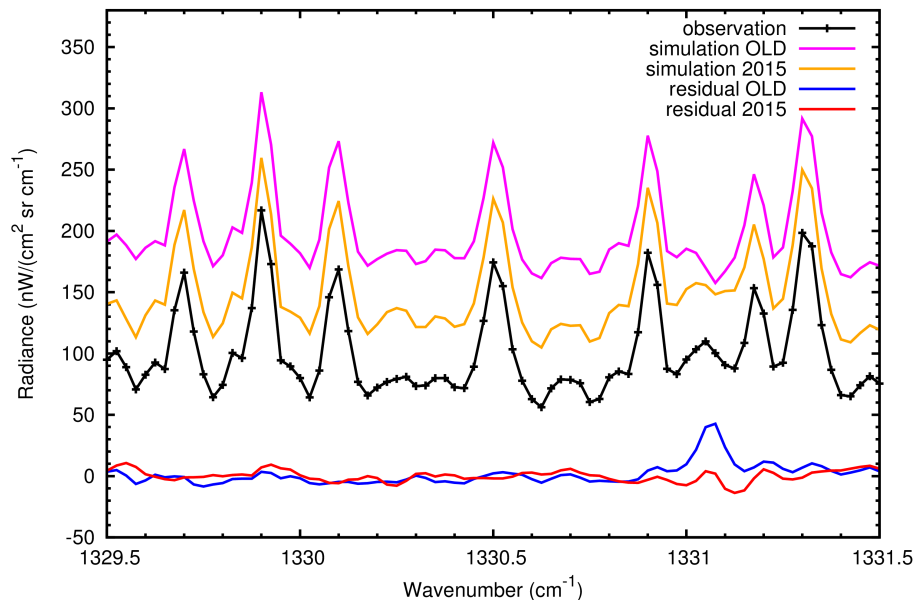


**Figure 5.** Average MIPAS observed spectrum (black) in the 1329.5–1331.5  $\text{cm}^{-1}$  spectral region, and simulated spectra with the MIPAS-OLD (magenta line) and the MIPAS-2015 (orange line)  $\text{HNO}_3$  line lists. For better readability of the plot, the average orange and magenta lines were shifted by 50 and 100  $\text{nW}(\text{cm}^2 \text{sr cm}^{-1})^{-1}$  respectively. The blue and the red lines are the residuals obtained with the MIPAS-OLD and the MIPAS-2015 line lists respectively.

[Title Page](#)[Abstract](#)[Introduction](#)[Conclusions](#)[References](#)[Tables](#)[Figures](#)[◀](#)[▶](#)[◀](#)[▶](#)[Back](#)[Close](#)[Full Screen / Esc](#)[Printer-friendly Version](#)[Interactive Discussion](#)

**MIPAS database: new  
HNO<sub>3</sub> line parameters  
at 7.6 μm validated  
with MIPAS satellite  
measurements**

A. Perrin et al.

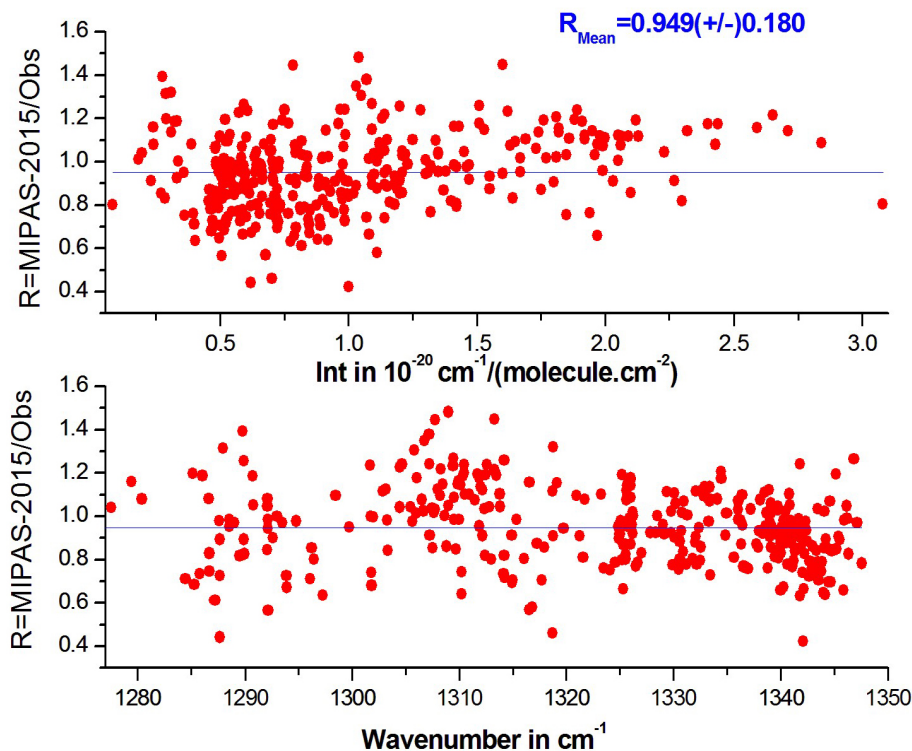


**Figure 6.** Comparison between the line intensities measured in this work using a Fourier transform spectrum (Obs, 299.7 K, 0.03 hPa, absorption path length = 302 cm, Perrin et al., 2004; Perrin 2013) and those available in MIPAS-2015. The comparison, performed as a function of the intensities and wavenumbers (upper and lower panels, respectively) accounts for the temperature correction from 299.7 to 296 K.

Title Page

Abstract

Introduction

Conclusions

References

Tables

Figures

◀

▶

◀

▶

Back

Close

Full Screen / Esc

Printer-friendly Version

Interactive Discussion



**MIPAS database: new  $\text{HNO}_3$  line parameters at 7.6  $\mu\text{m}$  validated with MIPAS satellite measurements**

A. Perrin et al.

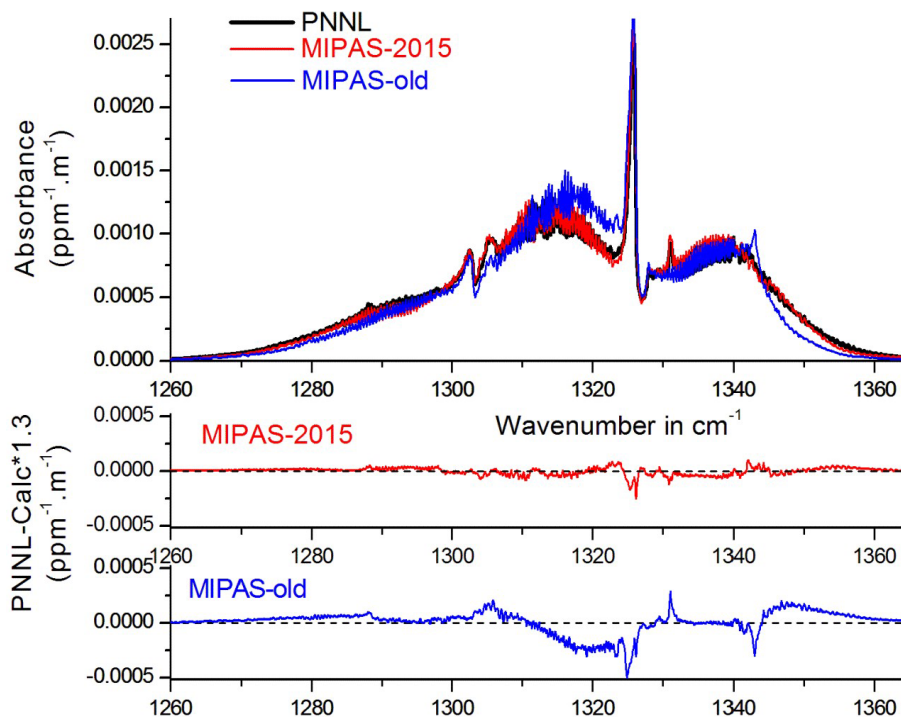


**Figure 7.** Upper panel: absorption cross sections from PNNL (Sharpe et al., 2004, black trace), and calculated using MIPAS-OLD (blue trace) and MIPAS-2015 (red trace); lower panel: corresponding residuals. For these calculations, the contributions of hot bands and bands from isotopologues other than  $\text{H}^{14}\text{N}^{16}\text{O}_3$  were accounted for by multiplying the calculated absorption cross sections by the ratio  $Z_{\text{vib}}(300\text{K})/I_a = 1.314$  (see Eq. 1).

[Title Page](#)[Abstract](#)[Introduction](#)[Conclusions](#)[References](#)[Tables](#)[Figures](#)[◀](#)[▶](#)[◀](#)[▶](#)[Back](#)[Close](#)[Full Screen / Esc](#)[Printer-friendly Version](#)[Interactive Discussion](#)